Effects of abrasive particle size and molecular weight of poly(acrylic acid) in ceria slurry on removal selectivity of SiO_2/Si_3N_4 films in shallow trench isolation chemical mechanical planarization

Hyun-Goo Kang
Nano-SOI Process Laboratory, Hanyang University, Seoul 133-791, Korea; and Division of Advanced Materials Science Engineering, Hanyang University, Seoul 133-791, Korea

Hyung-Soon Park
Hynix Semiconductor Inc., Icheon-si, Kyungki-do 467-701, Korea

Ungyu Paik[a)]
Division of Advanced Materials Science Engineering, Hanyang University, Seoul 133-791, Korea

Jea-Gun Park[b)]
Nano-SOI Process Laboratory, Hanyang University, Seoul 133-791, Korea

(Received 14 August 2006; accepted 13 December 2006)

The effects of the molecular weight and concentration of poly(acrylic acid) (PAA) with different primary abrasive sizes in ceria slurry on the nitride film loss, removal rate, film surface roughness, and removal selectivity of SiO_2-to-Si_3N_4 films were investigated by performing chemical mechanical polishing (CMP) experiments using blanket and patterned wafers. In the case of the blanket wafers, we found that for a lower PAA molecular weight, the removal selectivity of SiO_2-to-Si_3N_4 films increased more significantly with increasing PAA concentration in slurry containing a larger primary abrasive size. For the patterned wafers, with a higher PAA molecular weight in the ceria slurry suspension, the erosion of the Si_3N_4 film was less, but the removed amount was also smaller, and the surface roughness became worse after CMP. These results can be qualitatively explained by the layer of PAA adsorbed on the film surface, in terms of electrostatic interaction and rheological behavior.

I. INTRODUCTION

Chemical mechanical polishing (CMP) has emerged with rapid growth as a process for device fabrication in the semiconductor manufacturing industry, and it is expected to show further rapid growth as the device design rule shrinks. Specifically, the shallow trench isolation (STI) method, which has been used in advanced sub-250-nanometer integrated semiconductor device manufacturing, applies CMP to planarize gap-fill SiO_2 layers deposited on the front surfaces of wafers.[1,2] During the STI process, the active region where transistors are fabricated is generally covered with Si_3N_4 film.[3] The Si_3N_4 film acts as a mask for protection against reactive ion etching (RIE) during the trench formation step and as a barrier that stops the polishing process immediately after complete removal of the SiO_2 film. Ceria (CeO_2) slurries with organic additive are widely used in STI-CMP[4,5] because they have high removal selectivity of SiO_2 with respect to Si_3N_4 and widen the process margin in mass production. In addition to the high removal selectivity, ceria slurries also minimize the Si_3N_4 film loss while maintaining a high SiO_2 removal rate.[6,7] To achieve these benefits, however, the STI process itself must be optimized, and the material and consumable characteristics, such as the slurry performance and the nanoscale topography of the wafer surface and polishing pad, must be thoroughly investigated.[8–10]

To improve the performance of high-selectivity ceria slurry in STI-CMP, it is essential to control the slurry properties, including the pH, concentration, molecular weights of the organic additives, and abrasive particle size. We previously reported the effects of the pH and the concentration of organic additive in a ceria slurry suspension on improving the removal selectivity of SiO_2-to-Si_3N_4 films and the polishing rates for these films in CMP tests of blanket wafers.[11,12] We explained that the removal selectivity of SiO_2-to-Si_3N_4 films can be controlled by modifying the differences among the surface potentials of the abrasive particles, dispersant, and anionic

Address all correspondence to these authors.
[a)]e-mail: upaik@hanyang.ac.kr
[b)]e-mail: parkjgL@hanyang.ac.kr
DOI: 10.1557/JMR.2007.0097

organic additive in the ceria slurry, and those of the SiO_2 and Si_3N_4 film surfaces. The surface potentials are mainly affected by the suspension pH and the presence of dispersants and organic additives with different molecular weights. Hirai et al. explained the mechanism in terms of the selective adsorption of water-soluble acrylic polymers on SiO_2 and Si_3N_4 films, from which the characteristics of the passivation layers on the film surfaces are determined during the CMP process.[13] The selective adsorption has been attributed to the difference in surface zeta potentials between the SiO_2 and Si_3N_4 films.[14,15] Generally, the surface potentials of the SiO_2 film and the abrasive particles in ceria slurry with acrylate polymer are negatively charged and are above pH 3.0, while the Si_3N_4 film's surface potential is also negatively charged but is at least pH 7.0.[13–18] Philipossian et al. also proposed a selective adsorption model based on the zeta potential for the enhanced selectivity of ceria slurry with anionic organic polymer.[17] The attraction or repulsion between the abrasive particles and the films (SiO_2 and Si_3N_4) results from the different electrostatic potentials exhibited in certain pH regions. These differences affect the removal rates of the SiO_2 and Si_3N_4 films and hence the SiO_2-to-Si_3N_4 removal selectivity. To improve the removal selectivity of SiO_2-to-Si_3N_4 films by suppressing the Si_3N_4 removal, an anionic acrylic polymer is commonly used to protect the Si_3N_4 film.[18–20] Little is known, however, about methods of controlling the removal selectivity with respect to the SiO_2 and Si_3N_4 films. Furthermore, the complex effects of the molecular weight and the concentration of poly(acrylic acid) (PAA) in a ceria slurry suspension with different abrasive particle sizes on the correlation between the film removal rate and the SiO_2-and-Si_3N_4 removal selectivity in blanket and patterned wafer tests have not been reported.

Therefore, in this study, we investigated the dependencies of the removed amount and the surface roughness of SiO_2 and Si_3N_4 films on the molecular weight and the concentration of PAA in ceria slurries containing abrasives with different primary sizes, through STI-CMP tests using blank and patterned wafers.

II. EXPERIMENTAL

Cerium carbonate was used as a precursor to synthesize two types of ceria powder. The primary grain size of the polycrystalline ceria abrasives was controlled by employing a calcination process for 4 h with two different calcination temperatures, 700 and 800 °C. The secondary particle size of the abrasives was controlled by crushing the powders by using a laboratory-scale air jet mill and a wet ball mill. The ceria powders were crushed by wet mechanical milling for several hours to reduce their secondary particle sizes to the target size of 130 nm, after initial mechanical dry jet milling for several hours to reduce the size to 300 nm.[21] The ceria abrasives were then dispersed in deionized water and stabilized by adding 100 ppm of a commercially available dispersant [poly(methacrylate acid), PMAA], along with 1 wt% ammonium salt (molecular weight = 10,000; Darvan C, R.T Vandervilt, Norwalk, CT) as another dispersant of for the abrasive particles. We also added an anionic organic additive [poly(acrylic acid), PAA; Polysciences, Niles, IL] at a concentration of up to 0.80 wt%, with one of three different molecular weights (30,000, 50,000, and 90,000). Each suspension was twice subjected to ultrasonic treatment for 15 min to break down agglomerates and promote mixing. An ice bath was used to control the temperature of the suspension during the ultrasonic treatment. The suspension was aged for 12 h at room temperature with a wrist-action shaker and subjected to ultrasonic treatment for an additional 15 min prior to use. The solid content was initially controlled to 5 wt% ceria powder in the suspension. We then diluted each slurry with deionized water to produce a final ceria abrasive concentration of 1 wt%. Each slurry's pH was adjusted to the range of 6.0–7.0 by adding an alkaline agent. Table I lists the slurry characteristics, including the slurry pH, different PAA pH values with the three molecular weights, and experimental conditions during synthesis.

The crystal structure and grain size were analyzed with a diffractometer (RINT/DMAX-2500, Rigaku, Tokyo, Japan) using Cu-K_α radiation ($\lambda = 0.1542$ nm) at a scan rate of 2° min^{-1} (2θ min^{-1}). The intensity was logged over a 2θ range of 25~60 °C with a scan step of 0.02 °C. The grain sizes of the calcined powders were estimated using an x-ray line broadening method, by applying the Debye-Scherrer equation.[18] The morphology of the abrasives was observed with a high-resolution transmission electron microscope (HRTEM; JEM-2010, JEOL, Japan). The secondary particle size in each slurry was measured by acoustic attenuation spectroscopy (APS-100, Matec

TABLE I. Summary of slurry characteristics used in the experiment.

Sample	Slurry pH	Calcination temperature (°C)	Milling time (h)		Chemical additive characteristics		
			Dry	Wet	Concentration (wt%)	Molecular weight	pH
A	9.0	800	4	35	0–0.57	30,000	6.5
B	9.0	800	4	35	0–0.57	50,000	6.5
C	9.0	800	4	35	0–0.57	90,000	6.5
D	9.0	700	2	32	0–0.57	30,000	6.5

Applied Sc., Northborough, MA).[22] Each suspension pHwas measured with an advanced benchtop pH meter (Orion-525A, Thermo Orion, Beverly, MA) by adding KOH and HCl to control the range of 7.0–8.0. The rheological behavior of the slurry suspensions was examined with a controlled-stress viscometer (MCR300, Paar Physica, Ostfildem, Germany). This viscometer has a concentric-cylinder geometry, enabling us to investigate the stability behavior of the slurry with an external-temperature-control bath circulator operating at 25 ± 0.1 °C.

For blanket wafer tests, we used conventional 8-in. silicon wafers prepared by the single-side polishing method. SiO_2 films were deposited by the plasma-enhanced tetraethylorthosilicate (PETEOS) method. Si_3N_4 films were formed by low-pressure chemical vapor deposition (LPCVD). For the patterned case, the SKW-3 pattern wafer designed by SKW Associates (Santa Clara, CA) was used for characterization with respect to the pattern density and pitch size.[23,24] The STI mask consisted of 4 mm × 4 mm density and pitch structures dividing the 20 mm × 20 mm die into 5 rows and 5 columns. Figure 1 illustrates the specially designed layout of the SKW-3 pattern wafer, including (a) the pattern density and pitch size layout, (b) the mask floor plan, and (c) a cross-sectional view. The thicknesses of the as-deposited SiO_2 and Si_3N_4 films on the blanket and SKW-3 patterned wafers were 700 and 150 nm, respectively. In the density structure {where density is defined as the trench width (TW) / [TW + active width (AW)], or the trench area over the total area}, the pattern density is varied systematically from 0% to 100% in increments of 10%, with a fixed pitch of 100 um. The density structures are fabricated in a random layout to place high-density regions next to low-density regions. In the pitch structure, the density is fixed with the same trench width and space (50%), and the pitch is varied from 1 to 1000 μm, with vertically oriented lines. Cross-sectional pattern images of active Si_3N_4 and field SiO_2 layers before and after polishing were observed using scanning electron microscopy (SEM).

For the CMP process, the films were polished on a Strasbaugh 6EC polisher, with an IC1000/Suba IV stacked pad (Rodel, Newark, DE). The polishing pressure, applied as a down force, was 4 psi, equivalent to 27.5 kPa. The relative velocity between the pad and the wafer was 0.539 m/s. The polishing time was 30 s. The SiO_2 and Si_3N_4 film thickness variations of the wafers before and after CMP were measured with a NanoSpec 180 (Nanometrics, Milpitas, CA) and an Opti-probe (Therma-Wave, Fremont, CA). Cross-sectional images of the SKW-3 patterned wafers were obtained with a high-resolution scanning electron microscope (HRSEM; EP-1040, Hitachi, Tokyo, Japan). To analyze the surface roughness of the SiO_2 and Si_3N_4 films, an area of 1.0 μm × 1.0 μm was characterized with a commercial multimode

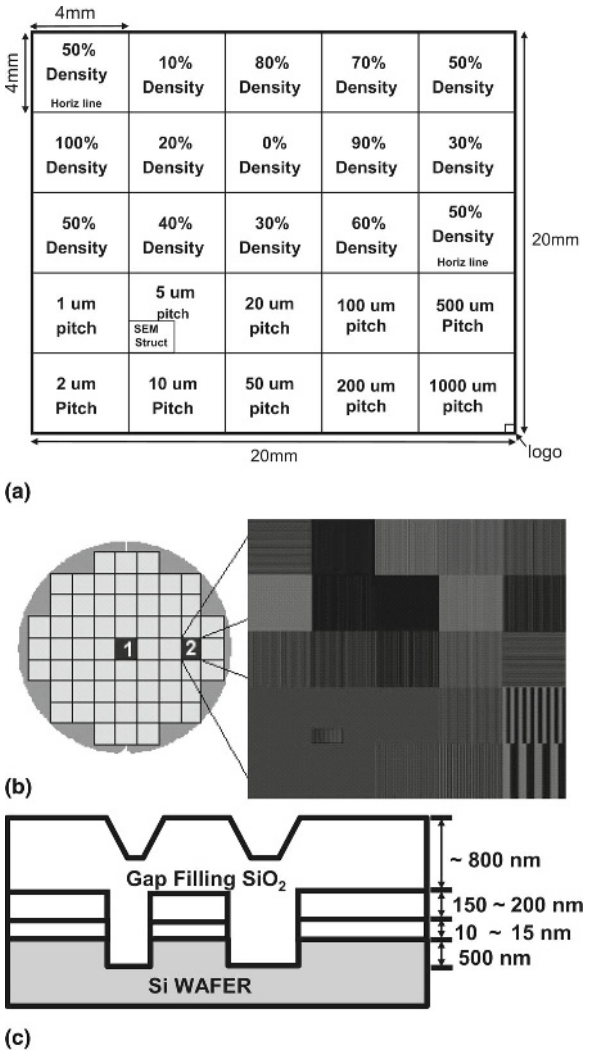

FIG. 1. Specially designed layout of the SKW-3 pattern wafer: (a) pattern density and pitch size layout, (b) mask floor plan, and (c) cross-sectional view.

atomic force microscope (AFM; XE 150, PSIA, Seungnam, Korea). A typical shallow trench structure was used to isolate the active regions where devices would be fabricated. The Si_3N_4 layer was attended, and a shallow trench was etched into the silicon, as illustrated in Fig. 2. A SiO_2 film was then deposited into the trench, resulting

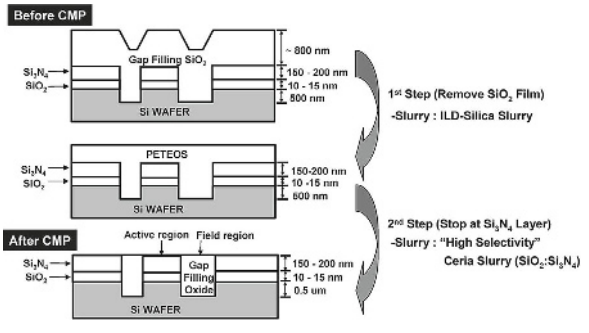

FIG. 2. Schematic process flow of a typical STI-CMP process.

in an overburden of SiO_2 above the Si_3N_4 active areas. In the ideal STI-CMP process in mass production, the SiO_2 film is removed roughly in all local step-coverage regions, leaving SiO_2 film only in the trench regions. Fumed silica slurry was used for the first CMP step, while the ceria slurries were used for the second CMP step in the polishing process to achieve stopping on the Si_3N_4 film surface after complete removal of the SiO_2 film.

III. RESULTS AND DISCUSSION

Figure 3 shows the HRTEM images and x-ray powder diffraction (XRD) patterns of the abrasive particles calcined at two different temperatures (700 and 800 °C). These images indicated that the primary grain size increased with calcination temperature and that the morphology of the ceria particle varied according to the calcination temperature. The abrasives calcined at 700 °C showed a relatively low crystallinity, whereas those calcined at 800 °C exhibited a relatively high crystallinity,

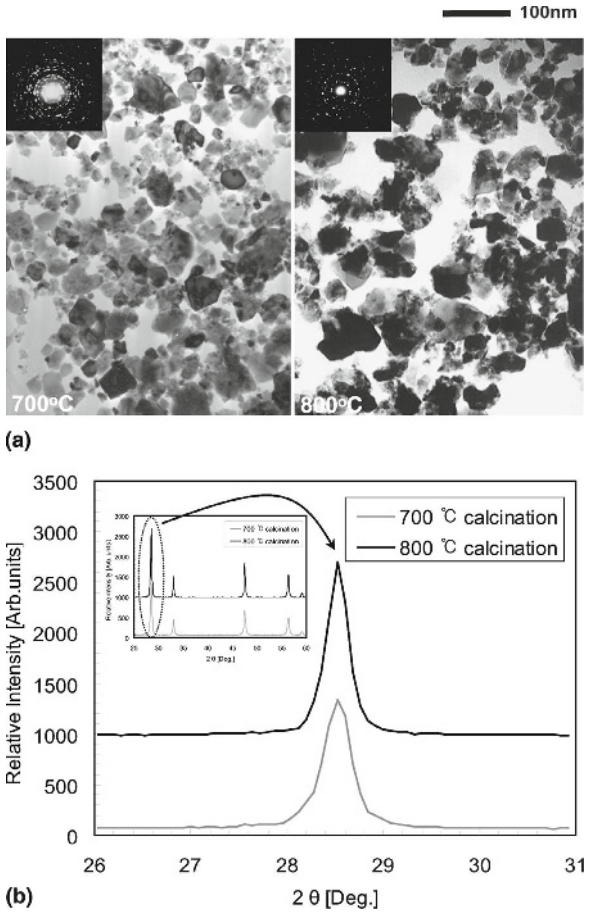

FIG. 3. HRTEM photograph and XRD powder diffraction patterns of the abrasive particles in a ceria slurry: (a) HRTEM photograph and diffraction pattern and (b) XRD powder diffraction pattern as a function of calcination.

and the shapes of the grain are well-defined, though some grains seem to contain sub-grain boundaries inside. In the ring-shaped diffraction, the particles calcined at temperatures as low as 700 °C still maintain their crystallinity as shown in Fig. 3(a). This result coincides with the XRD peaks shown in Fig. 3(b). In addition, the slurry calcined at 700 °C contains both medium-sized particles and many small primary particles, while the other slurry was composed of uniformly distributed, medium-sized particles. As confirmed by the TEM images, the slurry calcined at 700 °C had a wider size distribution than that of the other slurry. The XRD patterns of the powders calcined at different temperatures is shown in Fig. 3(b). Broader intensity peaks were observed for the ceria powders synthesized at 700 °C. This result may be considered by the low crystallinity with unreacted cerium carbonate and small-sized abrasive grains. The diffraction pattern shows only the peaks of cerium oxide with a fluorite structure; those for other compounds, such as cerium carbonate and cerous oxide, were not detected. With increased calcination temperature, the characteristic peaks of CeO_2 became sharper because the grains of single crystals were proportionally grown by heat treatment. This result affected the average grain size of the particles. The primary grain size of CeO_2 was investigated to clarify the relationship between the calcination temperature and the physical characteristics of the particles. The line-broadening of the (111) peak in XRD was analyzed to confirm the primary grain size of particles. The grain sizes of the particles were estimated using the Debye–Scherrer equation[18] by utilizing XRD line broadening as

$$D = 0.9\lambda/(\beta \cos \theta) \quad , \tag{1}$$

where λ is the wavelength of the monochromatic x-ray beam, θ is the diffraction angle, and β is the half-width of an intensity peak. The intensity peak at $2\theta = 28.2°$ was chosen for calculating the grain size, since it was clearer than any other peak and isolated from the others. The grain size moderately increased overall from 27 to 36 nm as the calcination temperature was increased from 700 to 800 °C, which can be attributed to thermally promoted grain growth[18,21] during the calcination process. These results are in agreement with the trend of increasing grain size in the TEM images shown in Fig. 3(a).

Figure 4(a) shows the distributions of the secondary particle sizes for both slurries without PAA addition. There was no difference in the distribution for small particle sizes of 0 to 0.6 um. On the other hand, the slurry calcined at 700 °C had a distribution with a higher range of large particles (>3 μm) than the other slurry. Figure 4(b) shows the median sizes (d_{50}) of the abrasives in each slurry as a function of the PAA concentration. With increasing PAA concentration, the average secondary particle size gradually increased within the concentration

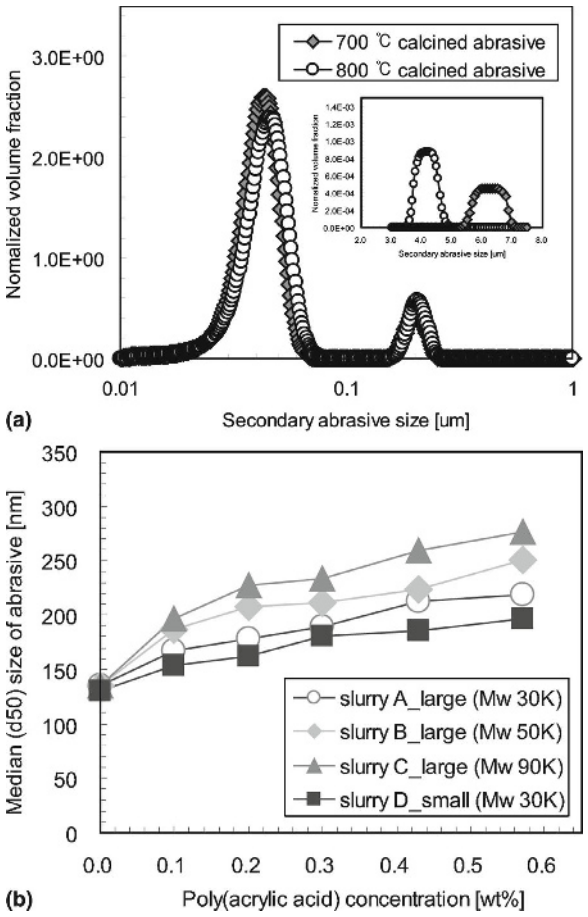

FIG. 4. (a) Abrasive particle size distribution without surfactant addition and (b) average median (d_{50}) abrasive size as a function of the surfactant molecular weight at pH 6.5–7.0.

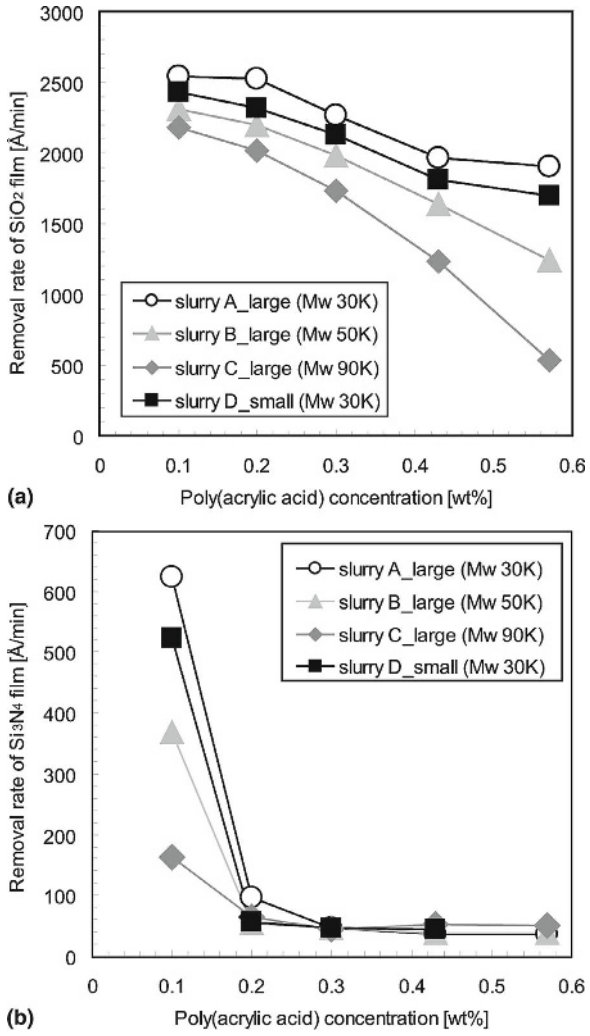

FIG. 5. Results of the CMP tests of blanket wafers in terms of the surfactant molecular weight: (a) removal rate of SiO_2 film and (b) removal rate of Si_3N_4 film.

range from 0 to 0.60 wt%. The average secondary particle size of the polycrystalline abrasives in ceria slurry is thought to be determined predominantly by PAA adsorption on the abrasives particle in the ceria slurry suspension. Generally, the amount of anionic PAA adsorbed on the abrasive particle surfaces, the configuration of the adsorbed PAA molecules, and the electric surface charge adsorbed from the particles by the PAA polymer chains control the agglomeration state and the stability of the dispersion.[11,14] Our previous report showed that the agglomeration of abrasives in the slurry occurs as the PAA concentration and the polycrystalline abrasive size are increased.[8–10] In the current study, we also confirmed that the order of the measured abrasive particle size (slurry D < A < B < C) did not change after PAA addition within the range from 0 to 0.60 wt%.

To evaluate the effects of the primary size of the ceria abrasives and the PAA concentration with different molecular weights on STI-CMP, we conducted blanket wafer tests and measured the removal rates of SiO_2 and Si_3N_4 for the three slurry samples. Figures 5(a) and 5(b) show the results obtained from a matrix experiment conducted by varying the molecular weights and concentrations of the PAA, along with the primary size of the ceria abrasives in each slurry. The removal rate of SiO_2 was reduced with increasing molecular weight for the same primary size throughout the experimental range of PAA concentrations, as shown in Fig. 5(a). For the PAA with the highest molecular weight with a different primary size, however, the removal rate of SiO_2 film was markedly reduced, from 2184 to 537 Å/min, as the PAA concentration increased. In contrast, in the case of the PAA with the lowest molecular weight, the removal rate was only slightly reduced, from 2542 to 1901 Å/min. Hence, with increasing PAA concentration, a higher primary abrasive size maintained a higher removal rate of SiO_2 at the same molecular weight. The removal rate of Si_3N_4 film versus the PAA concentration for slurries with the three different PAA molecular weights and the two primary abrasive sizes is shown in Fig. 5(b). We previously

reported that the contact probability of the abrasives on the film surface should strongly influence the removal rate.[25] We believe that the passivation layer is formed by PAA adsorbed on the film surface during CMP and that the effectiveness of this layer may depend on the amount of selective adsorption on the film surface and on the concentration of PAA with increased molecular weight.[11,26] Furthermore, we have attributed this to the behavior of abrasives moving in the PAA adsorption layer near the film surface. The removal rate of Si_3N_4 film was markedly reduced with increasing molecular weight, and it essentially saturated beyond a PAA concentration of 0.30 wt%. In addition, as a result of increasing the PAA concentration from 0.1 to 0.3 wt%, the slurries whose PAA had a medium or the lowest molecular weight maintained higher removal rates of Si_3N_4 film than did the slurry whose PAA had the highest molecular weight. In other words, with increasing PAA concentration and the addition of PAA having the same molecular weight, the removal rates of Si_3N_4 film for all slurries were markedly reduced, and they very quickly saturated at a higher molecular weight. By comparing Figs. 5(a) and 5(b), we can calculate the removal selectivity of the SiO_2-to-Si_3N_4 films. For the highest PAA molecular weight (MW = 90,000), the selectivity increased approximately from 10:1 to 13:1 with increasing PAA concentration. For the lowest molecular weight (MW = 30,000), however, the selectivity increased approximately from 4:1 to 51:1.

To clarify these results, the slurry samples were used in the STI planarization step for actual patterned wafers. Figure 6 shows the removed amounts of SiO_2 and Si_3N_4 films versus the pattern density of the patterned wafer for different PAA molecular weights and primary abrasive sizes. The SiO_2 film was fully over-polished with increasing pattern density, as shown in Fig. 6(a). The removed amount of Si_3N_4 film increased with increasing pattern density throughout the experimental range of PAA molecular weights on the concentration of 0.42 wt%, as shown in Fig. 6(b). In addition, as contrasted with the blanket wafer tests, with a higher PAA molecular weight and addition of the same PAA concentration, the removed amount of Si_3N_4 film in active regions was gradually reduced for all slurries. With a low PAA molecular weight, however, a smaller primary abrasive size maintained a higher removed amount of Si_3N_4 film at the same PAA molecular weight and concentration. In a previous study, we reported that the abrasive size influences the effect of the PAA on the removal rate of a ceria slurry.[25] We explained this result by using a model with the layer of PAA adsorbed or segregated on the film surface: larger abrasives are more likely to penetrate the viscous layer of adsorbed PAA, contact the hydrated surface, and form covalent bonds like Ce–O–Si on the film surface. According to this mechanism, the particle size

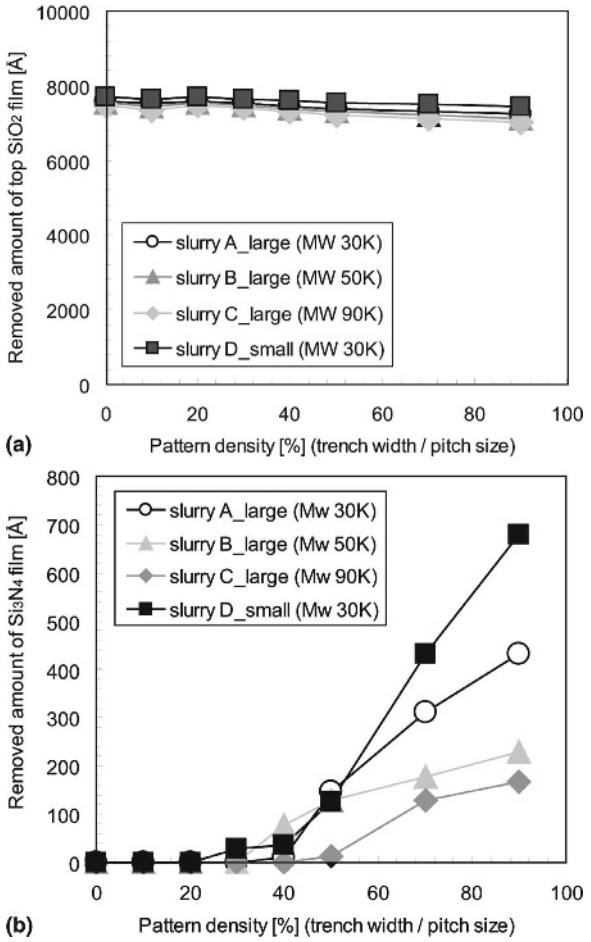

FIG. 6. Results of the CMP tests of patterned wafers in terms of the surfactant molecular weight: (a) removed amount of SiO_2 film and (b) removed amount of Si_3N_4 film.

determining the possibility of penetrating the viscous layer, contacting the hydrated film, and removing the film surface is one of the most important factors affecting the removal rate. As the particle size decreases, therefore, the removal rates also decrease. On the other hand, with many small particles remaining in the slurry suspension, whose surface areas are so large that they easily cause greater adsorption of PAA molecules in the slurry, the Si_3N_4 film can easily be removed because of the PAA adsorbed insufficiently on the densely separated Si_3N_4 film surface on a patterned wafer.

Figure 7 shows cross-sectional SEM images of the 5-μm pitch size with the density fixed at 50%, illustrating the edges of active Si_3N_4 and trench SiO_2 layers before and after polishing. With a higher PAA molecular weight and the same PAA concentration, the removed amount of Si_3N_4 film for all three slurries was gradually reduced with the narrow pitch size of 5 μm. The Si_3N_4 film erosion was clearly less for the PAA with the highest molecular weight, as compared to that for the low molecular weight. Hence, at the same molecular weight, a

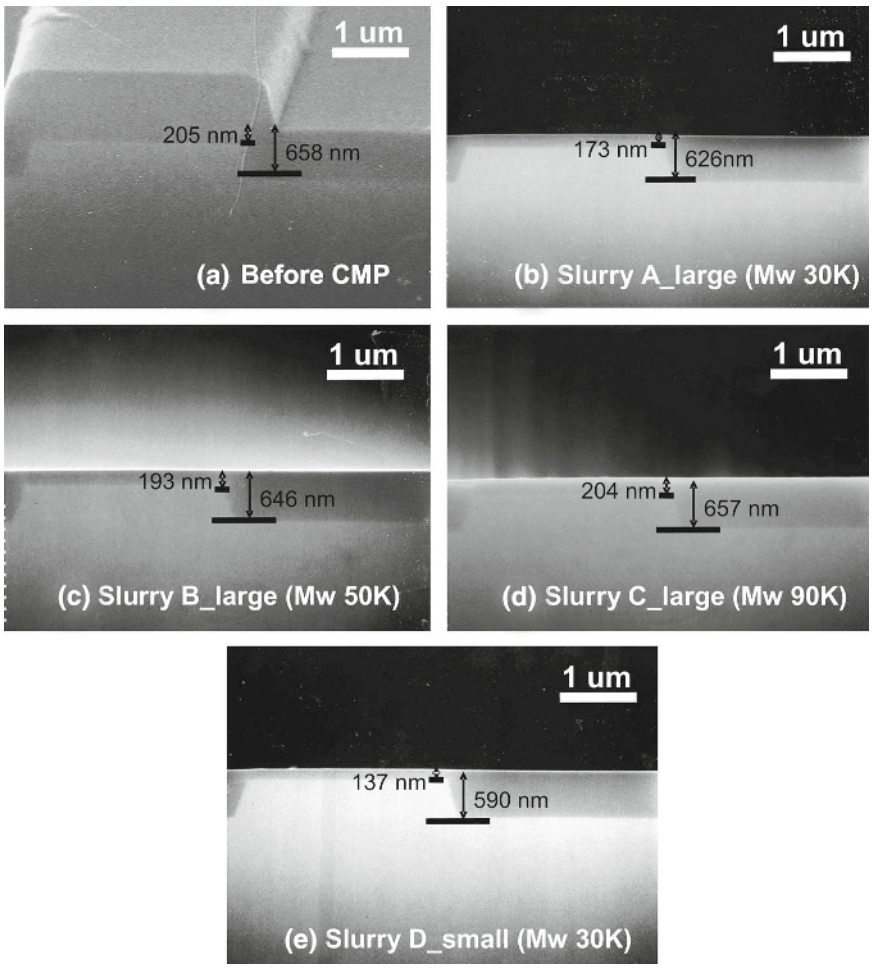

FIG. 7. Pre- and post-CMP cross-sectional SEM micrographs: (a) pre-CMP, (b) slurry A_large (molecular weight = 30,000), (c) slurry B_large (molecular weight = 50,000), (c) slurry C_large (molecular weight = 90,000), and (d) slurry D_small (molecular weight = 30,000).

smaller primary abrasive size maintained higher erosion of Si_3N_4 film than with a large primary size. The amount of PAA adsorption on the smaller particles was much higher than that on the larger particles because of their higher specific surface area, resulting in extra consumption of the PAA in the slurry solution. By comparing the images before and after CMP, we could calculate the amount of Si_3N_4 erosion. In this study, we also confirmed that the order of the measured Si_3N_4 film erosion [90 K (large) < 50 K (large) < 30 K (large) < 30 K (small)] did not change with respect to previous experimental results in this region with a low density of field Si_3N_4. These results are in good agreement with the Si_3N_4 film erosion shown in Fig. 6(b).

Figure 8(a) shows AFM line scan measurements indicating that a significant amount of SiO_2 local dishing occurred with over-polishing in a 500-μm-wide region. The dishing was reduced with increasing PAA molecular weight for the wide-field SiO_2 isolation region of 250 μm. Yu et al.[27] explained the mechanism of the dishing effect. For a narrow field width, the pressure exerted on the field SiO_2 is significantly reduced when the interface between the SiO_2 and Si_3N_4 films is reached in the CMP process, because the pressure applied by the pad is now concentrated on the Si_3N_4 layer as a result of its lower removal rate (about seven times lower than that of the field SiO_2).[27–30] In the wide-field region, the reduction in the local pressure is far less significant because of the elasticity of the pad, resulting in continued polishing of the field SiO_2 after the film interface (i.e., between field SiO_2 and active Si_3N_4) is reached during CMP, so that the wider the field region, the smaller the reduction in the pressure acting on the field SiO_2, and the greater the degree of dishing.[27] In our study, the dishing of the field SiO_2 was significantly lower because of the higher molecular weight of PAA in the ceria slurry, as shown in Fig. 8(a), which means that the PAA was more tightly adsorbed on the SiO_2 film because of the chain length and the chain bridging effect for the higher molecular weight than for the lower molecular weight.[11,16,31] It was found that the surface roughness of the active region was much higher for the PAA with the highest molecular

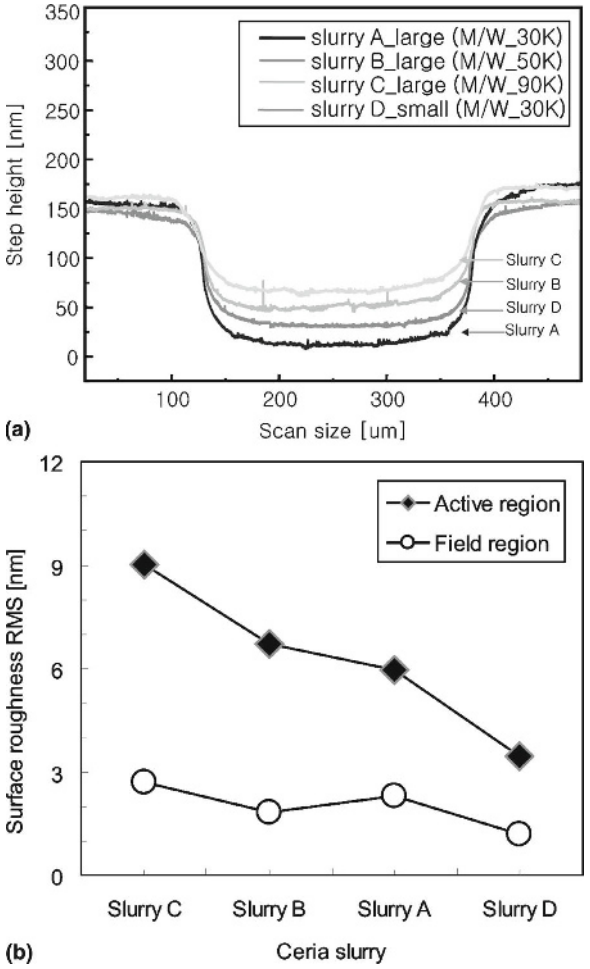

FIG. 8. (a) Post-CMP surface line scans of the wide-field SiO_2 region. (b) Post-CMP RMS surface roughness values.

weight than for that with the low molecular weight, as shown in Fig. 8(b). The surface roughness of the active Si_3N_4 region became worse with a higher molecular weight and the same primary abrasive size and PAA concentration, while a low value for the surface roughness of the field SiO_2 region was maintained. We previously reported, according to AFM analysis, that the adsorption of anionic PAA is attributed to the formation of a PAA adsorption layer on the Si_3N_4 film, as a result of the electrostatic interaction between the PAA and the film surface.[26]

The similar adsorption behavior of the PAA on the active Si_3N_4 films with a pattern density of 10% can be further characterized by the AFM images shown in Fig. 9. The morphology and surface roughness dependencies after polishing of the active Si_3N_4 region on the different PAA molecular weights and primary abrasive sizes were observed. In the case of the different primary sizes, there was no significant change in the film surface between the Si_3N_4 active surface and the adsorbed PAA after polishing. On the other hand, it was found that the surface roughness of the post-CMP Si_3N_4 film for the PAA with the highest molecular weight was much higher (0.355 nm) than that for the lowest molecular weight (0.280 nm), as illustrated in Figs. 9(a) and 9(d). This is attributed to the formation of the PAA adsorption layer on the Si_3N_4 film because of the electrostatic interaction between the PAA and the film surface. These results are in good agreement with the AFM line scan measurements shown in Fig. 8.

The adsorption behavior of the PAA on the ceria particles was mainly caused by the different surface charges

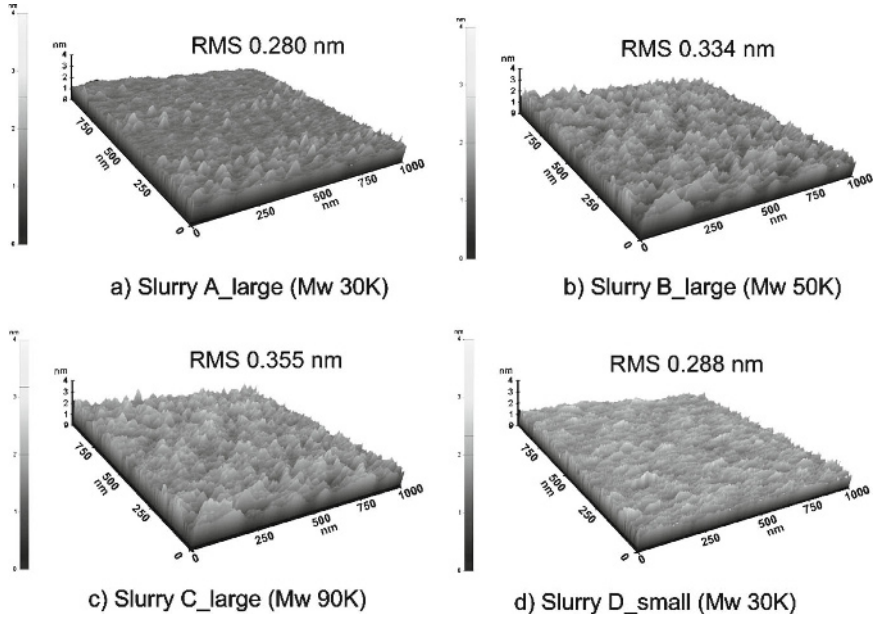

FIG. 9. Post-CMP three-dimensional AFM micrographs of patterned wafers: (a) slurry A_large (molecular weight = 30,000), (b) slurry B_large (molecular weight = 50,000), (c) slurry C_large (molecular weight = 90,000), and (d) slurry D_small (molecular weight = 30,000).

between the PAA and the ceria surface. The PAA is an anionic polyelectrolyte with an acidic carboxyl group, which leads to the ionization of the PAA molecules in the neutral pH region at which the ceria slurry for STI-CMP is usually manufactured.[14] Meanwhile, the net surface charge of the ceria particle is near zero in this pH region because the isoelectric point (pH_{iep}) of ceria is approximately 6–7.[11,14] Thus, the partially or fully ionized polyelectrolyte (PAA) is adsorbed on the ceria surface by electrostatic interactions.[14,18] The electrostatic attractive force between adsorbed PAA molecules on the water-particle interface and the Si_3N_4 film surface can be classified as mainly resulting from the electrostatic interaction of the electric double layer surrounding the particles and the steric hindrance effect of the adsorbed PAA molecules on the Si_3N_4 film.[22,32] Since the interaction of the electric double layer may have increased in proportion to the surface potential of absorbed PAA molecules with the same counter-ion content, the change in the zeta potential is important for the dependence of the electric double layer on the suspension properties. Moreover, the oxide film and the surface-modified ceria particles are negatively charged above pH 3, and the Si_3N_4 film is positively charged below pH 7. The attraction or repulsion between the abrasive particles and films (SiO_2 and Si_3N_4) results from the different electrostatic potentials exhibited in certain pH regions. Hence, during the blending of the slurry and additive solution, PAA that is used to form a passivation layer on the Si_3N_4 film can be additionally adsorbed on the surface of the ceria particles, which are basically covered by the same organic additive acting as the dispersant. This phenomenon could be explained as follows: the repulsive interaction between adjacent carboxyl sites is generated through the addition of more polymers, which then results in the conformational change of the adsorbed polymer.[14,33,34] In addition, the carboxylic acid group appear to be necessary to suppress the Si_3N_4 removal rate during CMP process through hydrogen bonding between Si_3N_4 film and carboxylic group in amino acid based ceria slurry. The electrostatic interactions between the abrasive particles in each slurry and the film surfaces, however, may not fully explain the suppressed removal rate of Si_3N_4 film and the removal selectivity of SiO_2-to-Si_3N_4 films with different PAA molecular weights. Hence, it is necessary to consider other factors that influence the abrasive movement in a slurry, from the point of view of rheological behavior. These factors depend on the passivation layer of PAA at the interface between the film surface and the ceria slurry suspension.

Figure 10 shows the rheological behaviors of various ceria slurries, with a fixed PAA pH of 7.0, as a function of the PAA concentration and molecular weight with different primary abrasive sizes. As shown in Fig. 10(a), for the PAA with the higher molecular weights, the slurry

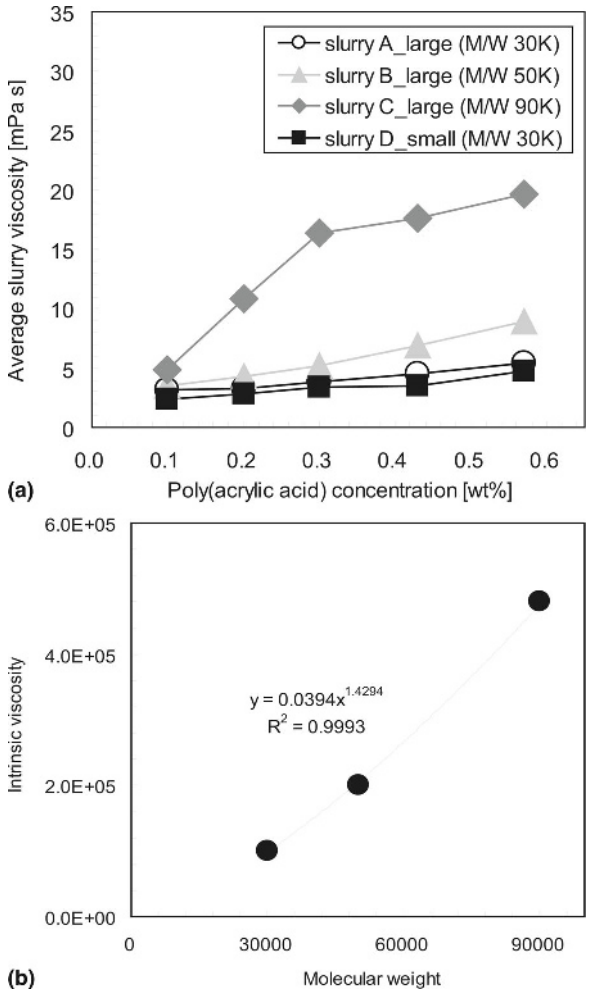

FIG. 10. Experimental slurry viscosity with surfactants of different molecular weights: (a) average slurry viscosity as a function of the surfactant concentration and molecular weight and (b) intrinsic viscosity calculated from Eqs. (1) and (2).

viscosity increased markedly with the PAA concentration, but it barely increased with the concentration in the case of the low molecular weight, regardless of the abrasive size. The primary abrasive size made no difference in the average slurry viscosity for the two different primary sizes. The measured effects of the PAA concentration and molecular weight on the slurry viscosity are in good agreement with results reported previously.[9,12] For the same weight concentration of ceria abrasives, the number of molecules in a ceria suspension with a higher molecular weight PAA will be lower than that with a lower molecular weight.

According to the Mark–Houwink–Sakurada equation,[35,36] the relationship between the viscosity, molecular weight, and organic polymer type can be formulated as

$$[\eta_i] = \mathrm{Km}\, M_w^{\ a} \quad , \tag{2}$$

where η_i is the intrinsic viscosity, a and Km are constants

for a specific polymer solvent system, and M_w is the average molecular weight of the polymer. The constant Km depends on primary molecular features, such as the persistence length, while a depends on short-range interactions and their implied effect on the molecular weight. For each slurry with a range of PAA molecular weights, the relation between the intrinsic viscosity and molecular weight is one of its most important properties. This relation can be represented by the following equation:

$$\ln \eta_i = \ln \mathrm{Km} + a \ln M_w \quad . \tag{3}$$

We calculated the parameters Km and a from a plot of ln η_i versus ln M_w, as shown in Fig. 10(b). For the constants in Eq. (2), we chose the values for PAA in a ceria slurry solution, enabling us to evaluate the average molecular weight of PAA in this solution. Here, the amount of PAA adsorption (or segregation on the surface) depends on the bulk concentration of the PAA and the electrostatic interaction between the PAA and the film surface. Moreover, because a PAA with a higher molecular weight adsorbs more densely, the intrinsic viscosity [η_i in Eq. (1)], which describes the particle behavior near the film surface, should increase and hinder the movement of particles. As a result, the removal rates of both the SiO_2 and the Si_3N_4 films were reduced as the molecular weight and the concentration of the PAA increased in the blanket wafer tests. Moreover, the removal rates of the SiO_2 and Si_3N_4 films can become important, depending on the passivation layer of PAA existing at the interface. Thus, the addition of a PAA with a lower molecular weight appears to passivate the electrostatic interactions, thereby resulting in weaker adhesion of the adsorbed PAA layer through polymer chain bridging and branching,[36–40] and possibly resulting in desorption of this layer above a certain applied load during the CMP process. As the PAA chain length increases, however, the lateral interaction among the hydrocarbon chains becomes more pronounced, resulting in the formation of a more effectively passivated layer of PAA. Consequently, with increasing PAA concentration and addition at a higher molecular weight, the Si_3N_4 removal rates for all slurries markedly reduced in the blanket wafer tests. Although in the case of a higher PAA molecular weight, the removal rate and erosion of Si_3N_4 film could be reduced, for a patterned wafer, the removal rate of the field SiO_2 film was also reduced, while the surface roughness of the Si_3N_4 film in the active region was increased.

The chemical factors can be either increased or reduced through certain additives, according to the above mechanism, thus resulting in a corresponding CMP rate modulation. Therefore, this study has provided key information regarding the PAA molecular weight in ceria slurry for STI-CMP, explaining that the reduced removal rate of Si_3N_4 film, as well as the SiO_2 removal rate, surface roughness, and so forth, are very important parameters for successful implementation of STI-CMP. The proposed mechanism of PAA molecular weight in STI-CMP has been inferred to explain our data and observations. Without any possible real-time monitoring of the adsorption behavior of PAA on the Si_3N_4 and SiO_2 films during the CMP process, however, the mechanism is not comprehensively proven, and it may not cover all situations. Further efforts toward in situ CMP monitoring are thus strongly recommended.

IV. CONCLUSIONS

In summary, we have systematically investigated shallow trench isolation using the CMP process with ceria slurry containing anionic organic additive (PAA) and different primary abrasive sizes, PAA molecular weights, and PAA concentrations. We have also examined the impacts of the removal selectivity, erosion, dishing, and surface roughness of SiO_2 and Si_3N_4 films. For the PAA with the highest molecular weight in our experiments using blanket wafer, with different primary abrasive sizes, the removal rates of the SiO_2 and Si_3N_4 films were markedly reduced as the PAA concentration increased. Hence, with increasing PAA concentration, a higher primary abrasive size maintained a higher removal rate of SiO_2 at the same PAA molecular weight and concentration. For the case of patterned wafers, with a higher PAA molecular weight, the erosion of Si_3N_4 film could be reduced, but our pattern wafer tests showed that the removal amount was reduced and the surface roughness of the Si_3N_4 film became worse. These results can be qualitatively explained from the layer of PAA adsorbed on the film surface in terms of electrostatic interaction and rheological behavior, including the molecular weights, concentrations of PAA, and different primary abrasive sizes in the ceria slurry.

ACKNOWLEDGMENTS

The Korea Ministry of Science & Technology supported this work through the National Research Laboratory (NRL) program. We thank Sumitomo Mitsubishi Silicon Corp. and Hynix Semiconductor, Inc. for helping us with our experiments. We are also indebted to Mr. Manabu Kanemoto, Mr. Jin-Hyung Park, Mr. Jun-Seok Kim, Mr. Byong-Seog Lee, and Mr. Hyuk-Yul Choi for assisting us in performing the experiments.

REFERENCES

1. S. Wolf: *Silicon Processing for the VLSI Era: Process Integration,* Vol. 2, (Lattice Press, Sunset Beach, CA, 1990), Chap. 13, p. 24.
2. M. Quirk and J. Serda: *Semiconductor Manufacturing Technology* (Prentice Hall, NJ, 2001), Chap. 9, p. 199.

3. J.Y. Cheng, T.F. Lei, and T.S. Chao: A novel shallow trench isolation technique. *Jpn. J. Appl. Phys.* **36,** 1319 (1997).
4. H.S. Park, K.B. Kim, C.K. Hong, U.I. Chung, and M.Y. Lee: Control of microscratches in chemical-mechanical polishing process for shallow trench isolation. *Jpn. J. Appl. Phys.* **37,** 5849 (1998).
5. T. Hoshino, Y. Kurata, Y. Terasaki, and K. Susa: Mechanism of polishing of SiO_2 films by CeO_2 particles. *J. Non-Cryst. Solids* **283,** 129 (2001).
6. H. Nojo, M. Kodera, and R. Nakata: Slurry engineering for self-stopping, dishing free SiO_2-CMP, Proc. IEEE Idem, San Francisco, CA, 1996 (The Institute of Electrical and Electronics Engineers, Piscataway, NJ, 1996), p. 349.
7. J.Y. Kim, S.K. Kim, U. Paik, T. Katoh, and J.G. Park: Effect of crystallinity of ceria particles on the PETEOS removal rate in chemical mechanical polishing for shallow trench isolation. *J. Kor. Phys. Soc.* **41,** 413 (2002).
8. H.G. Kang, T. Katoh, H.S. Park, U. Paik, and J.G. Park: Effects of abrasive size of polycrystalline nano ceria slurry on shallow trench isolation chemical mechanical polishing. *Jpn. J. Appl. Phys.* **43,** L365 (2004).
9. H.G. Kang, T. Katoh, W.M. Lee, U. Paik, and J.G. Park: Dependence of nanotopography impact on abrasive size and surfactant concentration in ceria slurry for shallow trench isolation chemical mechanical polishing. *Jpn. J. Appl. Phys.* **43,** L1 (2004).
10. J.G. Park, T. Katoh, H.C. Yoo, D.H. Lee, and U. Paik: Spectral analyses on pad dependency of nanotopography impact on oxide chemical mechanical polishing. *Jpn. J. Appl. Phys.* **41,** L17 (2002).
11. H.G. Kang, M.Y. Lee, H.S. Park, U. Paik, and J.G. Park: Dependence of pH, molecular weight, and concentration of surfactant in ceria slurry on saturated nitride removal rate in shallow trench isolation chemical mechanical polishing. *Jpn. J. Appl. Phys.* **44,** 4752 (2005).
12. H.G. Kang, T. Katoh, H.S. Park, U. Paik, and J.G. Park: Dependence of non-Prestonian behavior of ceria slurry with anionic surfactant on the abrasive concentration and size in shallow trench isolation chemical mechanical polishing. *Jpn. J. Appl. Phys.* **44,** 4752 (2006).
13. K. Hirai, H. Ohtsuki, T. Ashizawa, and Y. Kurata: High performance CMP slurry for STI. *Hitachi Chem. Tech. Report* **35,** 17 (2000).
14. S.K. Kim, S. Lee, U. Paik, T. Katoh, and J.G. Park: Influence of the electrokinetic behaviors of abrasive ceria particles and the deposited plasma-enhanced tetraethylorthosilicate and chemically vapor deposited Si_3N_4 films in an aqueous medium on chemical mechanical planarization for shallow trench isolation. *J. Mater. Res.* **18,** 2163 (2003).
15. W.G. America and S.V. Babu: Slurry additive effects on the suppression of silicon nitride removal during CMP. *Electrochem. Solid-State Lett.* **7,** G327 (2004).
16. L. Wang, W.M. Sigmund, and F. Aldinger: Systematic approach for dispersion of silicon nitride powder in organic media: II. Dispersion of the powder. *J. Am. Ceram. Soc.* **83,** 697 (2000).
17. A. Philipossian and M. Hanazono: Tribology and fluid dynamics characterization of cerium oxide slurries. www.innovative-planarization.com. (2001).
18. S.K. Kim, P.H. Yoon, U. Paik, T. Katoh, and J.G. Park: Influence of physical characteristics of ceria particles on polishing rate of chemical mechanical planarization for shallow trench isolation. *Jpn. J. Appl. Phys.* **43,** 7427 (2004).
19. Y.Z. Hu, R.J. Gutmann, and T.P. Chow: Silicon nitride chemical mechanical polishing mechanism. *J. Electrochem. Soc.* **145,** 3919 (1998).
20. S.D. Kim, I.S. Hwang, and H.M. Park: Chemical mechanical polishing of shallow trench isolation using the ceria-based high selectivity slurry for sub-0.18 μm complementary metal-oxide-semiconductor fabrication. *J. Vac. Sci. Technol. B* **20,** 918 (2002).
21. D.H. Kim, H.G. Kang, S.K. Kim, U. Paik, and J.G. Park: Effect of calcination process on synthesis of ceria particles, and its influence on STI CMP performance. *Jpn. J. Appl. Phys.* **45,** 4893 (2006).
22. V.A. Hackley: Colloidal processing of silicon nitride with poly (acrylic acid): I, adsorption and electrostatic interactions. *J. Am. Ceram. Soc.* **80,** 2315 (1997).
23. D. Boning, B. Lee, C. Oji, D. Ouma, T. Park, T. Smith, and T. Tugbawa: Pattern dependent modeling for CMP optimization and control, in *Chemical-Mechanical Polishing–Fundamentals and Challenges,* edited by S.V. Babu, S. Danyluk, M. Krishnan, and M. Tsujimura (Mater. Res. Soc. Symp. Proc. **566,** Warrendale, PA, 2000), P5.5, p. 761.
24. D. Boning and B. Lee: Nanotopography issues in shallow trench isolation CMP. *MRS Bull.* **27**(10), 761 (2002).
25. T. Katoh, H.G. Kang, U. Paik, and J.G. Park: Effects of abrasive morphology and surfactant concentration on polishing rate of ceria slurry. *Jpn. J. Appl. Phys.* **42,** 1150 (2003).
26. C.W. Cho, S.K. Kim, J.G. Park, W.M. Sigmund, and U. Paik: Atomic force microscopy study of the role of molecular weight of poly(acrylic acid) in chemical mechanical planarization for shallow trench isolation. *J. Mater. Res.* **21,** 473 (2006).
27. C. Yu, P.C. Fazan, V.K. Mathews, and T.T. Doan: Dishing effects in a chemical mechanical polishing planarization process for advanced trench isolation. *Appl. Phys. Lett.* **61,** 1344 (1992).
28. J.M. Boyd and J.P. Ellul: Near-global planarization oxide-filled shallow trenches using chemical mechanical polishing. *J. Electrochem. Soc.* **143,** 3718 (1996).
29. B.A. Bonner, A. Iyer, D. Kumar, T.H. Osterheld, A.S. Nickles, and D. Flynn: Development of a direct polish process for shallow trench isolation modules, in *Chemical Mechanical Planarization for ULSI Multilevel Interconnection* (CMP-MIC Spring Meeting, 2001), p. 572.
30. S.S. Cooperman, A.I. Nasr, and G.J. Grula: Optimization of a shallow trench isolation process for improved planarization. *J. Electrochem. Soc.* **142,** 3180 (1995).
31. G.B. Basim and B.M. Boudgil: Role of interaction forces in controlling the stability and polishing performance of CMP slurries. *J. Colloid Interface Sci.* **256,** 137 (2002).
32. U. Paik, V.A. Hackley, J. Lee, and S. Lee: Effect of poly(acrylic acid) and poly(vinyl alcohol) on the solubility of colloidal $BaTiO_3$ in an aqueous medium. *J. Mater. Res.* **18,** 1266 (2005).
33. P.W. Carter and T.P. Johns: Interfacial reactivity between ceria and silicon dioxide and silicon nitride surfaces. *Electrochem. Solid-State Lett.* **8,** G221 (2005).
34. K. Rajan, R. Singh, J. Adler, U. Mahajan, Y. Rabinovich, and B. Moudgil: Surface interaction forces in chemical-mechanical polishing. *Thin Solid Films* **308–309,** 529 (1997).
35. H. Togrul and N. Arslan: Flow properties of sugar beet pulp cellulose and intrinsic viscosity-molecular weight relationship. *Carbohydrate Polym.* **54,** 63 (2003).
36. Q. Shen, D. Mu, L.W. Yu, and L. Chen: A simplified approach for evaluation of the polarity parameter for polymer using the K coefficient of the Mark–Houwink–Sakurada equation. *J. Colloid Interface Sci.* **275,** 30 (2004).
37. J.S. Reed: *Principles of Ceramics Processing*, 2nd ed. (Wiley Interscience, New York, 1995), Chap. 17, p. 323.
38. R.J. Hunter: *Introduction to Modern Colloid Science* (Oxford University Press Inc., New York, 1993), Chap. 1, p. 204.
39. F.W. Billmeyer: *Textbook of Polymer Science* (Wiley Interscience, New York, 1984), p. 7.
40. S. Choibowski and M. Wisniewska: Study of electrokinetic properties and structure of adsorbed layers of polyacrylic acid and polyacrylamide at Fe_2O_3-polymer solution interface. *Colloids Surf. A* **208,** 131 (2002).